New Avian Hepadnavirus in Palaeognathous Bird, Germany

Wendy K. Jo,[1] Vanessa M. Pfankuche,[1] Henning Petersen, Samuel Frei, Maya Kummrow, Stephan Lorenzen, Martin Ludlow, Julia Metzger, Wolfgang Baumgärtner, Albert Osterhaus, Erhard van der Vries

Author affiliations: University of Veterinary Medicine Hannover, Foundation, Hannover, Germany (W.K. Jo, V.M. Pfankuche, H. Petersen, M. Ludlow, J. Metzger, W. Baumgärtner, A. Osterhaus, E. van der Vries); Center for Systems Neuroscience, Hannover (W.K. Jo, V.M. Pfankuche, W. Baumgärtner, A. Osterhaus); Wuppertal Zoo, Wuppertal, Germany (S. Frei, M. Kummrow); Bernhard Nocht Institute for Tropical Medicine, Hamburg (S. Lorenzen); Artemis One Health, Utrecht, the Netherlands (A. Osterhaus)

DOI: https://doi.org/10.3201/eid2312.161634

In 2015, we identified an avian hepatitis B virus associated with hepatitis in a group of captive elegant-crested tinamous (*Eudromia elegans*) in Germany. The full-length genome of this virus shares <76% sequence identity with other avihepadnaviruses. The virus may therefore be considered a new extant avian hepadnavirus.

Hepatitis B virus (HBV) belongs to the family *Hepadnaviridae*, members of which constitute 2 major extant genera: *Orthohepadnavirus*, which infect mammals, and *Avihepadnavirus*, which infect birds (*1*). Recently, evidence of a likely third genus was found with the discovery of a new fish hepadnavirus (*2*). In addition, HBV-derived endogenous viral elements have been reported in several neoavian birds (e.g., budgerigars and several finches) (*3,4*) and reptiles (e.g., turtles and crocodiles) (*5*).

Hepadnaviruses generally are characterized by their narrow host range and strong hepatotropism (*1*). They are enveloped, partially double-stranded DNA viruses with a small circular genome (≈3 kb) and at least 3 open reading frames (ORFs) (*1*). In orthohepadnaviruses, a fourth ORF encodes the X protein, which is associated with hepatocellular carcinoma in their respective host species. Avihepadnaviruses appear to have an X-like protein region; however, either a premature stop codon is present or no ORF is found in most cases (*6*). We describe a new avian HBV causing severe hepatitis in the elegant-crested tinamou (*Eudromia elegans*), a member of the ancient group of birds the Palaeognathae, which includes emus (*Dromaius novaehollandiae*) and ostriches (*Struthio* spp.).

In 2015, a deceased adult elegant-crested tinamou kept at Wuppertal Zoo (Wuppertal, Germany) underwent necropsy at the University of Veterinary Medicine Hannover, Foundation (Hannover, Germany). Initial histologic examination revealed moderate, necrotizing hepatitis and inclusion body–like structures within the hepatocytes. To identify a putative causative agent, we isolated nucleic acids from the liver and prepared them for sequencing on an Illumina MiSeq system (Illumina, San Diego, CA, USA) (online Technical Appendix, https://wwwnc.cdc.gov/EID/article/23/12/16-1634-Techapp1.pdf). We compared obtained reads with sequences in GenBank using an in-house metagenomics pipeline. Approximately 78% of the reads aligned to existing avihepadnavirus sequences. A full genome (3,024 bp) of the putative elegant-crested tinamou HBV (ETHBV) was subsequently constructed by de novo assembly mapping >2 million reads (88.6%) to the virus genome (GenBank accession no. KY977506).

The newly identified ETHBV shared <76% nt sequence identity with other avian HBVs (online Technical Appendix Table 1). Phylogenetic analysis showed that ETHBV clustered within the genus *Avihepadnavirus*, forming a new clade (Figure, panel A). The organization of the ETHBV genome was similar to other avian HBVs because all 3 overlapping ORFs (polymerase, nucleocapsid [preC/C], and presurface [preS/S] antigen) and several essential sequence motifs (e.g., the epsilon element, TATA boxes, and direct repeat sites DR1 and DR2) were identified (online Technical Appendix Figure 1). We also found an X-like sequence. However, similar to duck HBV, ETHBV lacks a putative translation start site. It has been suggested that the X protein evolved later in mammalian hosts (*5*), which explains the absence of X-like ORF in the ETHBV genome. Comparison of pairwise amino acid identities between ETHBV and other avihepadnaviruses showed low homologies between their functional proteins (64%–69% similarity to the polymerase, 75%–80% to the preC/C, 52%–62% to the preS/S [online Technical Appendix Table 2]).

The identification of ETHBV prompted us to retrospectively screen the flock of 7 elegant-crested tinamous at Wuppertal Zoo and the 6 that had died within the past 4 years and had undergone necropsy at the University of Veterinary Medicine Hannover, Foundation (online Technical Appendix Table 4). For that purpose, we designed a set of degenerated primers targeting a short region of the polymerase–preC/C genome in all avihepadnaviruses (online Technical Appendix). All birds were found positive by PCR (online Technical Appendix Table 4), including liver tissue from embryonated eggs, implying that ETHBV is vertically transmitted (Figure, panel B). We then obtained a second ETHBV genome (GenBank accession

[1]These authors contributed equally to this article.

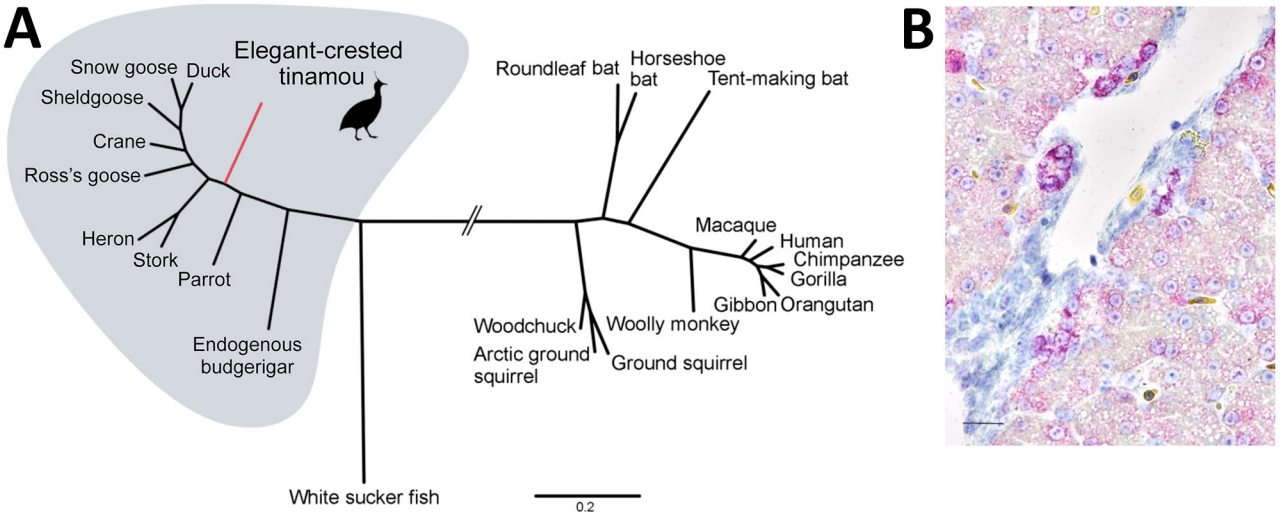

Figure. Phylogenetic and histopathologic analysis of probable new avian hepadnavirus, elegant-crested tinamou hepatitis B virus (ETHBV), Germany. A) Bayesian phylogeny of virus isolated from an elegant-crested tinamou (*Eudromia elegans*) compared with reference viruses. Tree was created on the basis of full-genome sequences from the family *Hepadnaviridae*. The analysis was run for 4 million generations and sampled every 100 steps, and the first 25% of samples were discarded as burn-in in MrBayes (*7*). Hasegawa-Kishino-Yano nucleotide substitution model was selected as best-fit model according to Bayesian information criteria. Posterior probabilities are shown in online Technical Appendix Figure 3 (https://wwwnc.cdc.gov/EID/article/23/12/16-1634-Techapp1.pdf). Branches were truncated for graphical reasons (interrupted lines). GenBank accession number for isolates, is available online (http://wwwnc.cdc.gov/EID/article/23/16-1634-F1.htm). Scale bar indicates nucleotide substitutions per site. B) ETHBV-specific RNA (in red; Fast Red) localized within hepatocytes of the liver tissue of an elegant-crested tinamou embryo by in situ hybridization (online Technical Appendix). Positive signal is enhanced in hepatocytes localized close to the vessels and negative in endothelial cells. Nonprobe incubation of the tinamou and liver tissue from a pheasant were used as negative controls. Scale bar indicates 40 μm.

no. KY977507) from another tinamou from the same flock by deep sequencing; this genome showed 99.8% nt sequence identity with the initial ETHBV genome. Tinamou serum samples from another zoo were also screened but tested negative by PCR (online Technical Appendix Table 4).

To further characterize ETHBV, we confirmed infection in the liver using an in situ hybridization protocol (*8*) in an adult and embryo tinamou (Figure, panel B). In addition to ETHBV infection in the liver, we found some positive cells in kidney and testis tissue. Although hepadnaviruses generally are host restricted, exceptions have been reported (e.g., crane HBV) (*9*). We attempted to infect Pekin duck embryos through the allantoic cavity, as well as by intravenous infection routes, and were not able to demonstrate replication (data not shown).

ETHBV can be considered a new extant hepadnavirus associated with hepatitis in the elegant-crested tinamou. Whether ETHBV can infect other species within the Palaeognathae or whether it is host restricted within other tinamou species remains to be elucidated. The discovery of ETHBV suggests that other avian species may harbor as-yet undiscovered HBVs. The pathogenesis of avian hepadnavirus infections and the mechanisms of virus transmission in captive tinamou flocks warrant further investigation.

Acknowledgments

We thank Mareike Schubert, Kerstin Rohn, Danuta Waschke, Bettina Buck, Caroline Schütz, Kerstin Schöne, Heike Klippert-Hasberg, Mogens Drabert, Stefan Neander, and Jörn Wrede for excellent technical assistance. We also are grateful to Severin Dressen and Emile Prins for their collaboration in the project.

This study was in part supported by a grant from the Niedersachsen-Research Network on Neuroinfectiology from the Ministry of Science and Culture of Lower Saxony, Germany. This study also was in part supported by the COMPARE project and received funding from the European Union's Horizon 2020 research and innovation program COMPARE (grant agreement no. 643476).

Dr. Jo is a PhD candidate at the University of Veterinary Medicine Hannover Research Center for Emerging Infections and Zoonoses, Hannover, Germany. Her research interests include virus discovery, emerging and re-emerging infections, cross-species transmission, viral evolution, and host adaptation.

References

1. Funk A, Mhamdi M, Will H, Sirma H. Avian hepatitis B viruses: molecular and cellular biology, phylogenesis, and host tropism. World J Gastroenterol. 2007;13:91–103. http://dx.doi.org/10.3748/wjg.v13.i1.91

2. Hahn CM, Iwanowicz LR, Cornman RS, Conway CM, Winton JR, Blazer VS. Characterization of a novel hepadnavirus in the white sucker (Catostomus commersonii) from the Great Lakes region of the United States. J Virol. 2015;89:11801–11. http://dx.doi.org/10.1128/JVI.01278-15
3. Liu W, Pan S, Yang H, Bai W, Shen Z, Liu J, et al. The first full-length endogenous hepadnaviruses: identification and analysis. J Virol. 2012;86:9510–3. http://dx.doi.org/10.1128/JVI.01164-12
4. Suh A, Brosius J, Schmitz J, Kriegs JO. The genome of a Mesozoic paleovirus reveals the evolution of hepatitis B viruses. Nat Commun. 2013;4:1791. http://dx.doi.org/10.1038/ncomms2798
5. Suh A, Weber CC, Kehlmaier C, Braun EL, Green RE, Fritz U, et al. Early mesozoic coexistence of amniotes and hepadnaviridae. PLoS Genet. 2014;10:e1004559. http://dx.doi.org/10.1371/journal.pgen.1004559
6. Chang SF, Netter HJ, Hildt E, Schuster R, Schaefer S, Hsu YC, et al. Duck hepatitis B virus expresses a regulatory HBx-like protein from a hidden open reading frame. J Virol. 2001;75:161–70. http://dx.doi.org/10.1128/JVI.75.1.161-170.2001
7. Huelsenbeck JP, Ronquist F. MRBAYES: Bayesian inference of phylogenetic trees. Bioinformatics. 2001;17:754–5. http://dx.doi.org/10.1093/bioinformatics/17.8.754
8. Pfankuche VM, Bodewes R, Hahn K, Puff C, Beineke A, Habierski A, et al. Porcine bocavirus infection associated with encephalomyelitis in a pig, Germany. Emerg Infect Dis. 2016;22:1310–2. http://dx.doi.org/10.3201/eid2207.152049
9. Prassolov A, Hohenberg H, Kalinina T, Schneider C, Cova L, Krone O, et al. New hepatitis B virus of cranes that has an unexpected broad host range. J Virol. 2003;77:1964–76. http://dx.doi.org/10.1128/JVI.77.3.1964-1976.2003

Address for correspondence: Erhard van der Vries, Department of Infectious Diseases & Immunology, Faculty of Veterinary Medicine, Section Virology, Utrecht University, Utrecht, the Netherlands; email: e.vandervries@uu.nl

Acute Myopericarditis Associated with Tickborne *Rickettsia sibirica mongolitimonae*

Pablo Revilla-Martí, Álvaro Cecilio-Irazola, Jara Gayán-Ordás, Isabel Sanjoaquín-Conde, Jose Antonio Linares-Vicente, José A. Oteo

Author affiliations: Hospital Clínico Universitario Lozano Blesa, Zaragoza, Spain (P. Revilla-Martí, A. Cecilio-Irazola, J. Gayán-Ordás, I. Sanjoaquín-Conde, J.A. Linares-Vicente); Centro de Investigación Biomédica de La Rioja, Logroño, Spain (J.A. Oteo)

DOI: https://doi.org/10.3201/eid2312.170293

We report an unusual case of myopericarditis caused by *Rickettsia sibirica mongolitimonae*. Because of increasing reports of *Rickettsia* spp. as etiologic agents of acute myopericarditis and the ease and success with which it was treated in the patient reported here, rickettsial infection should be included in the differential diagnosis for myopericarditis.

Myopericarditis is a primarily pericardial inflammatory syndrome occurring when clinical diagnostic criteria for pericarditis are satisfied and concurrent mild myocardial involvement is documented by elevated biomarkers of myocardial damage (i.e., increased troponins). Limited clinical data on the causes of myopericarditis suggest that viral infections are among the most common causes in developed countries, although the list of agents is increasing. We identified an unusual case of myopericarditis caused by *Rickettsia sibirica mongolitimonae*, an emerging pathogen in southern Europe with a broad clinical spectrum (*1*).

In September 2016, a 39-year-old man with no remarkable medical history sought care at an emergency department in Spain with acute-onset central chest pain and fever. The previous week, he had hunted in northeastern Spain. Physical examination revealed a systolic blood pressure of 115 mm Hg, heart rate 80 beats/min, peripheral pulse oximetry of 98%, and an axillary temperature of 38.7°C. No murmurs, rales, or gallops were detected on cardiac examination. A necrotic left gluteus eschar and multiple enlarged left inguinal lymph nodes were noted. He had neither lymphangitis nor widespread rash, and his mucous membranes appeared normal. He did not remember tick bites.

An electrocardiogram demonstrated a sinus rhythm with diffuse ST-segment elevation, and a transthoracic echocardiogram showed a normal biventricular ejection fraction with mild pericardial effusion. High-sensitive T troponin level was 575.3 ng/L (reference <14 ng/L), and blood cultures and serologic tests for common viruses were all negative. He was admitted to the hospital, and a cardiac magnetic resonance study performed 48 hours later confirmed the suspected diagnosis of myopericarditis.

Because of the eschar, tickborne-related rickettsiosis was suspected, and ibuprofen (1,800 mg/d) and doxycycline (100 mg every 12 h) were started. After the third day on medical therapy, the patient became afebrile, and the electrocardiographic changes gradually resolved. He was discharged after 12 days. Doxycycline was maintained for 14 days.

Acute-phase serologic tests yielded negative results for HIV; *Borrelia burgdorferi* sensu lato (chemiluminiscence immunoassay, Liason, Diasorin, Spain); spotted fever group rickettsia (SFGR) (commercial [Focus Diagnostics, Cypress, CA, USA] and in-house tests); and *Francisella tularensis* (in-house microagglutination assay). An eschar swab sample and an eschar biopsy sample were removed under aseptic

Article DOI: https://doi.org/10.3201/eid2312.161634

New Avian Hepadnavirus in Palaeognathous Bird, Germany

Technical Appendix

Sample Preparation and Sequencing

Virus enrichment procedures were applied to the liver tissue before DNA and RNA extractions. Briefly, after homogenization, 3 cycles of freeze/thaw were applied, followed by host nucleic acids degradation with OmniCleave endonuclease (Epicenter Biotechnologies, Madison, WI, USA). RNA and DNA were extracted following TRIzol and the QIAamp DNA mini Kit (Qiagen, Hilden, Germany) procedures, respectively. Next, nucleic acids were randomly amplified using a modified sequence-independent single-primer amplification protocol (*1*) in which random hexamers were replaced by nonribosomal hexamers (*2*). Library preparation was performed following Nextera XT DNA Sample Preparation Kit protocol (Illumina, San Diego, CA, USA). Samples were then sequenced on an Illumina MiSeq sequencer with the MiSeq Reagent Kit v3 (300 × 2 cycles). De novo assembly was performed using the software CLC Genomics Workbench 8.0.3 (https://www.qiagenbioinformatics.com/products/clc-genomics-workbench/).

Detection of Avihepadnaviruses by Quantitative PCR

Oligonucleotides were designed targeting conserved regions between 78 avian hepatitis B viruses (HBVs) aligned genome sequences, including elegant-crested tinamou hepatitis B virus (ETHBV). The resulting forward primer ATTGAAGCAATCACTmGACCAmTCC and reverse primer CTTwGAACGTCTTCTCCCATAGAC amplify a 137-bp fragment within the polymerase and nucleocapsid regions. Quantitative PCR (qPCR) reactions consisted of 1 μL of DNA template, 1× SYBR green mix (Agilent, Santa Clara, CA, USA), 250 nM of forward and reverse primers, making a total of 20 μL reaction volume. The amplification protocol used was as follows: 95°C for 3 min, 40 cycles of 95°C for 10 s, 50°C for 10 s, and 60°C for 10 s in a

qPCR instrument. A melting curve was generated following 1 cycle of 35°C for 30 s, 60°C for 30 s, and 95°C for 30 s. The qPCR sensitivity was evaluated using 10-fold dilution series of ETHBV DNA samples (Technical Appendix Table 3). Moreover, FFPE-positive liver tissues and a negative control (chicken embryo fibroblast cells) samples were also tested.

Amplification of ETHBV Full Genome

Full genome of ETHBV was obtained by conventional PCR using abutting primers (ETHBV_fw: ATGATGCAGGAATCCTTTATAAGCGAG; ETHBV_rv: AAAGCTTAGTTAAATATTCCCCAACTATCTCC) targeting the polymerase region (Technical Appendix Figure 1). PCR reactions consisted of 1 μL of DNA template, 1× buffer, 200 nM dNTPs, 0.5 μM forward and reverse primers, and 1U of Phusion polymerase (New England Biolabs, Ipswich, MA, USA), making 50 μL of total reaction volume. Amplification protocol used was as follows: 98°C for 30 s, 35 cycles of amplification (98°C for 30 s, 64°C for 1 min, and 72°C for 2 min), and a final extension of 72°C for 10 min. A full genome of 3,024 bp was amplified (Technical Appendix Figure 3). Moreover, positive band was cut and purified followed by a digestion with *Eco*RI.

In situ Hybridization

In situ hybridization (ISH) targeting regions of the polymerase and presurface antigen of ETHBV (GenBank accession no. KY977506) was performed on formalin-fixed, paraffin-embedded liver section, according to the manufacturer's protocol (ViewRNA ISH Tissue 1-Plex Assay Kit and ViewRNA Chromogenic Signal Amplification Kit, Affymetrix-Panomics, Santa Clara, CA, USA) with minor variations, as formerly described (*3*).

GenBank Accession Numbers in the Figure

Elegant-crested tinamou, KY977506; woodchuck, AY334076; woolly monkey, AF046996; gibbon, U46935; orangutan, EU155826; gorilla, FJ798096; chimpanzee, D00220; human, AB775200; macaque, HE815465; horseshoe bat, KC790377; roundleaf bat, KC790373; tent-making bat, KC790378; Arctic ground squirrel, U29144; ground squirrel, K02715;

endogenous budgerigar, BK008521; duck, X60213; snow goose, AF110996; sheldgoose, AY494853; crane, AJ441111; Ross's goose, M95589; parrot, JN565944; heron, M22056; stork, AJ251935.

References

1. Allander T, Tammi MT, Eriksson M, Bjerkner A, Tiveljung-Lindell A, Andersson B. Cloning of a human parvovirus by molecular screening of respiratory tract samples. Proc Natl Acad Sci U S A. 2005;102:12891–6. PubMed http://dx.doi.org/10.1073/pnas.0504666102

2. Endoh D, Mizutani T, Kirisawa R, Maki Y, Saito H, Kon Y, et al. Species-independent detection of RNA virus by representational difference analysis using non-ribosomal hexanucleotides for reverse transcription. Nucleic Acids Res. 2005;33:e65. PubMed http://dx.doi.org/10.1093/nar/gni064

3. Pfankuche VM, Bodewes R, Hahn K, Puff C, Beineke A, Habierski A, et al. Porcine bocavirus infection associated with encephalomyelitis in a pig, Germany. Emerg Infect Dis. 2016;22:1310–2. PubMed http://dx.doi.org/10.3201/eid2207.152049

Technical Appendix Table 1. Full genome nucleotide sequence identity between prototype avianhepadnaviruses and the new elegant-crested tinamou hepatitis B virus*

Bird	GenBank accession no.	Elegant-crested tinamou	Duck	Snow goose	Sheldgoose	Crane	Ross's goose	Heron	Stork	Parrot
Elegant-crested tinamou	KY977506	100								
Duck	X60213	74.0	100							
Snow goose	AF110996	74.4	89.2	100						
Sheldgoose	AY494853	73.4	85.0	84.7	100					
Crane	AJ441111	75.9	83.3	83.2	83.2	100				
Ross's goose	M95589	75.1	81.3	80.3	80.5	84.1	100			
Heron	M22056	72.1	76.1	76.0	75.4	77.0	76.6	100		
Stork	AJ251935	72.6	76.2	76.6	76.5	78.6	77.1	85.3	100	
Parrot	JN565944	71.1	73.8	74.0	73.9	74.9	74.0	73.3	73.5	100

*Sequence identities presented as percentages.

Technical Appendix Table 2. Homologies between the different proteins of prototype avihepadnaviruses and the elegant-crested tinamou hepatitis B virus*

Bird	GenBank accession no.	Polymerase	PreC/C	PreS/S	X-like
Duck	X60213	68	75	60	57
Snow goose	AF110996	69	76	61	61
Sheldgoose	AY494853	68	76	57	64
Crane	AJ441111	68	76	62	65
Ross's goose	M95589	68	76	60	61
Heron	M22056	64	79	60	56
Stork	AJ251935	65	80	59	59
Parrot	JN565944	65	78	52	59

*Homologies between amino acid sequences are presented in percentages. PreC/C, nucleocapsid antigen; PreS/S, presurface antigen.

Technical Appendix Table 3. ETHBV DNA samples for evaluating quantitative PCR using SYBR green probe*

Sample	Cycle threshold	Melting temperature
ETHBV	11	81.0
ETHBV 1×10^{-1}	14	81.0
ETHBV 1×10^{-2}	18	81.0
ETHBV 1×10^{-3}	23	81.0
ETHBV 1×10^{-4}	25	81.0
ETHBV FFPE	18	80.5
CEF	>30	75.5
NTC	>30	75.5

*ETHBV, elegant-crested tinamou; FFPE, formalin-fixed paraffin-embedded; CEF, chicken embryo fibroblast cells; NTC, negative template control.

Technical Appendix Table 4. Avihepadnavirus qPCR detection in elegant-crested tinamou samples from Wuppertal Zoo (Germany) and GaiaZOO (Netherlands)*

Identifier	Zoo	Status	Histopathologic diagnosis of liver	Sample	C_t	Tm
101-160014	Wuppertal	Dead (died 05/2015)	Hepatitis, necrotizing, moderate, multifocal with intralesional, intranuclear inclusion body-like structures	Liver	10	81.0
				FFPE-Liver	18	80.5
407-160049	Wuppertal	Dead (died 11/2013)	Hepatitis, lymphohistiocytic, mild, oligofocal	Liver	13	81.0
				Lung	15	81.0
				Kidney	19	81.0
				Brain	20	81.0
407-160050	Wuppertal	Dead (died 06/2015)	Hepatitis, lymphohistiocytic, partially suppurative to pyogranulomatous, moderate, multifocal	Liver	7	81.0
				Lung	17	81.0
				Kidney	12	81.0
				Spleen	16	81.0
				Brain	23	81.0
				Intestines	18	81.0
407-160051	Wuppertal	Dead (died 03/2016)	Hepatocellular necrosis, mild, multifocal; hepatitis, lymphohistiocytic, mild, multifocal; hepatocellular vacuolization, mild, diffuse	Liver	8	81.0
				Lung	13	81.0
				Kidney	14	81.0
				Spleen	16	81.0
407-160052	Wuppertal	Dead (died 04/2016)	Hepatitis, necrotizing, moderate, multifocal with intralesional, intranuclear inclusion body-like structures; hemorrhage, moderate, focal, acute	Liver	7	81.0
				Lung	No C_t	81.0
				Kidney	15	81.0
				Brain	18	81.0
				Muscle	19	81.0
407-160053	Wuppertal	Dead (died 05/2016)	Not done	Egg yolk	16	81.0
				Liver	18	81.0
407-160054	Wuppertal	Dead (died 05/2016)	Not done	Egg yolk	13	81.0
				Liver	9	81.0
407-160056	Wuppertal	Alive	Not applicable	Serum	8	81.0
407-160057	Wuppertal	Alive	Not applicable	Serum	9	81.0
407-160058	Wuppertal	Alive	Not applicable	Serum	10	81.0
407-160059	Wuppertal	Alive	Not applicable	Serum	9	81.0
407-160060	Wuppertal	Alive	Not applicable	Serum	12	81.0
407-160376	Wuppertal	Alive	Not applicable	Serum	9	81.0
407-160377	Wuppertal	Alive	Not applicable	Serum	10	81.0
412-160374	GaiaZOO	Alive	Not applicable	Serum	>30	76.0
412-160375	GaiaZOO	Alive	Not applicable	Serum	>30	76.0
412-160376	GaiaZOO	Alive	Not applicable	Serum	>30	76.0

*qPCR, quantitative PCR; C_t, cycle threshold; Tm, melting temperature; negative: Tm ≠ 81 and C_t >30; positive: Tm = 81 and C_t ≤30.

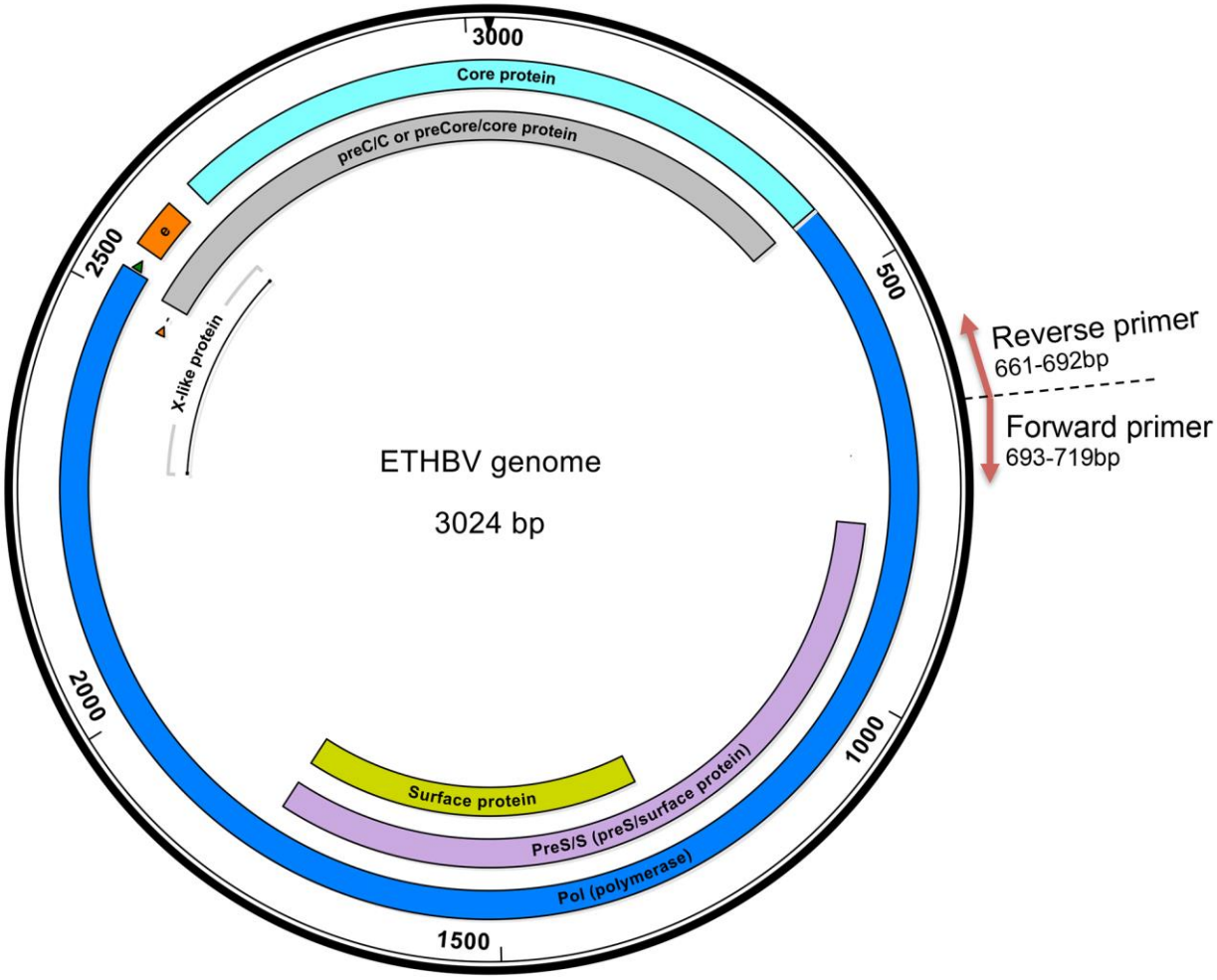

Technical Appendix Figure 1. Abutting primers design for the amplification of ETHBV full-genome representation. The annotated genome contains the coding proteins at the sites 170–2533 bp for the polymerase, 2521–3024, 1–414 bp for the preC/C, 2650–3024, 1–414 bp for the core, 801–1790 bp for the preS/S, and 1290–1790 bp for the surface; an X-like protein within 2292–2636 bp; direct repeat sequences DR1 and DR2 within 2537–2548 bp and 2480–2491 bp, respectively; and the epsilon motive (e) in the region 2563–2619bp. ETHBV, elegant-crested tinamou hepatitis B virus; preC/C, nucleocapsid antigen; preS/S, presurface antigen.

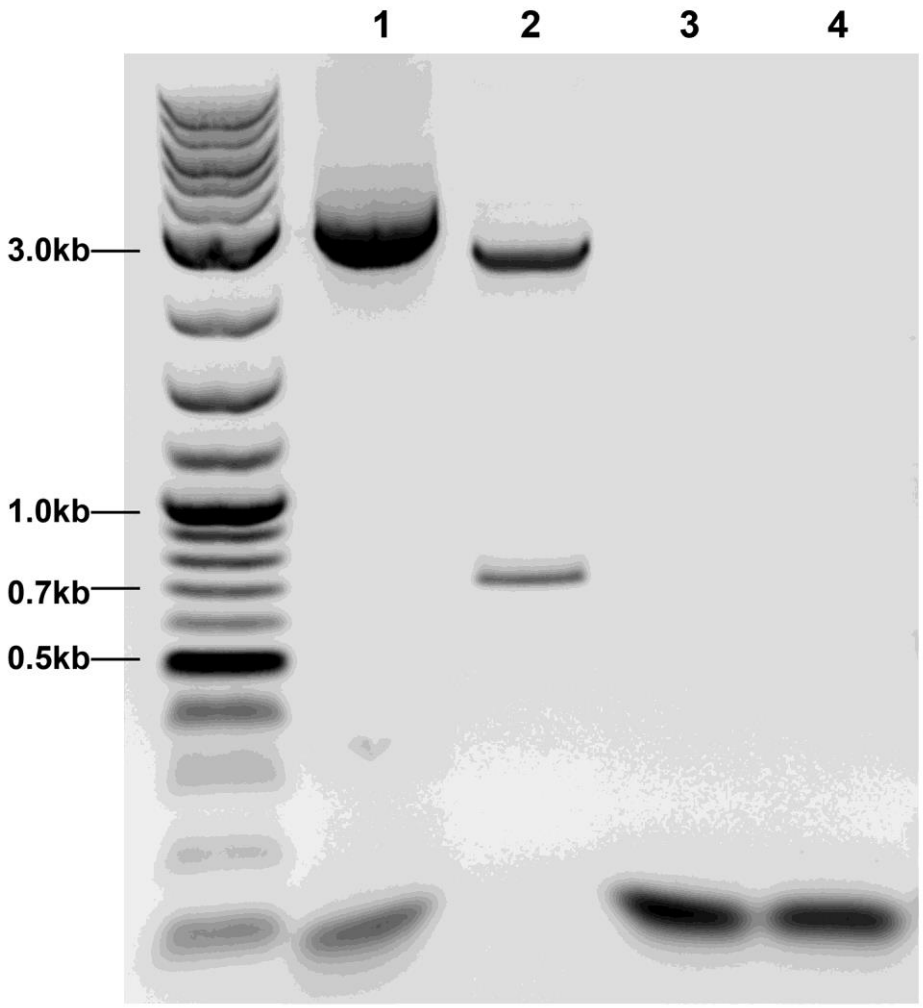

Technical Appendix Figure 2. Elegant-crested tinamou hepatitis B virus (ETHBV) full-genome amplification visualized on a 1% agarose gel. 1) Positive ETHBV sample: expected band at 3024 bp. 2) Digestion of ETHBV with *Eco*RI: expected bands at 696 bp and 2328 bp. 3) Negative control: tinamou serum from GaiaZOO 4) No template control.

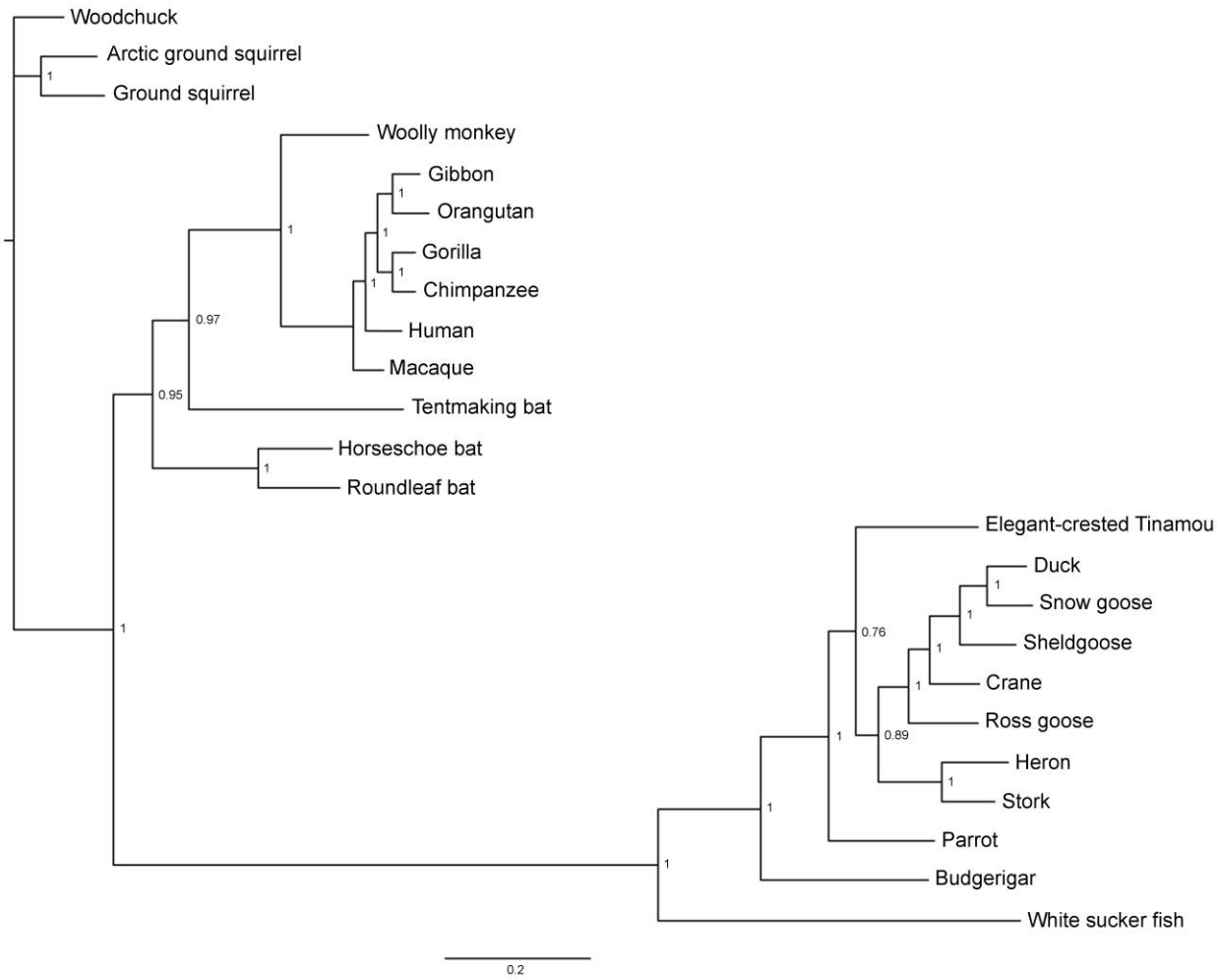

Technical Appendix Figure 3. Bayesian phylogeny with posterior probabilities based on full-genome sequences from the family *Hepadnaviridae*. The analysis was run for 4 million generations and sampled every 100 steps with the first 25% of samples discarded as burn-in in MrBayes. Hasegawa-Kishino-Yano nucleotide substitution model was selected as best-fit model according to Bayesian information criteria. Scale bar indicates nucleotide substitution per site. GenBank accession numbers of hepadnaviruses: woodchuck, AY334076; woolly monkey, AF046996; gibbon, U46935; orangutan, EU155826; gorilla, FJ798096; chimpanzee, D00220; human, AB775200; macaque, HE815465; horseshoe bat, KC790377; roundleaf bat, KC790373; tent-making bat, KC790378; Arctic ground squirrel, U29144; ground squirrel, K02715; endogenous budgerigar, BK008521; duck, X60213; snow goose, AF110996; sheldgoose, AY494853; crane, AJ441111; Ross's goose, M95589; parrot, JN565944; heron, M22056; stork, AJ251935; elegant-crested tinamou, KY977506.